Lymphatic PD-L1 expression restricts tumor-specific CD8$^+$ T cell responses

Stefan Cap[1,*], Manuel Dihr[1,*], Nikola Cousin[1], Carlotta Tacconi[1], Michael Detmar[1,2], Lothar C. Dieterich[1,2]

[1] Institute of Pharmaceutical Sciences, Swiss Federal Institute of Technology (ETH) Zurich, Zurich, Switzerland

[2] Correspondence:

michael.detmar @pharma.ethz.ch

lothar.dieterich@pharma.ethz.ch

* equal contribution

Running title: Lymphatic PD-L1 restrains tumor immunity

ABSTRACT

Lymph node (LN)-resident lymphatic endothelial cells (LECs) mediate peripheral tolerance by presentation of self-antigens on MHC-I and constitutive expression of T cell inhibitory molecules, including PD-L1. PD-L1 is also induced in tumor-associated LECs but the specific role of lymphatic PD-L1 in tumor immunity has remained unknown. We generated a mouse model lacking lymphatic PD-L1 expression and challenged these mice with two orthotopic tumor models, B16F10 melanoma and MC38 colorectal carcinoma. Lymphatic PD-L1 deficiency resulted in a consistent expansion of tumor-specific $CD8^+$ T cells in tumor-draining LNs in both tumor models and increased the efficacy of adoptive T cell therapy in the B16F10 model. Strikingly, lymphatic PD-L1 primarily acted via apoptosis induction in tumor-specific $CD8^+$ central memory T cells. Our findings demonstrate that LECs restrain tumor-specific immunity via PD-L1 and may explain why some cancer patients without PD-L1 expression in the tumor microenvironment still respond to PD-L1 / PD-1 targeting immunotherapy.

INTRODUCTION

Lymphatic vessels play an essential role in the generation of adaptive immune responses, providing a transport route for antigen and antigen-presenting cells (APCs) from peripheral tissues to secondary lymphoid organs such as lymph nodes (LNs), and for freshly primed lymphocytes from the LNs to the central circulation. Likewise, within the LNs, lymphatic sinuses orchestrate the lymph flow, antigen entry into the parenchyma, and immune cell migration. Lymphatic endothelial cells (LECs) that line all lymphatic vessels and sinuses have recently emerged as direct, antigen-dependent and independent regulators of adaptive immunity, in particular of dendritic cells (DCs) and T cells [1,2]. LN-residing LECs for instance express and present peripheral tissue self-antigens on MHC-I [3,4], and thereby inhibit autoreactive T cells specific for those antigens [5,6]. They are also able to sample free antigen from the lymph and cross-present it on MHC-I under steady-state conditions [7]. Thus, LN LECs have been suggested as important contributors to the maintenance of peripheral self-tolerance. On the other hand, LN LECs may also stimulate memory differentiation in a subset of T cells [8] and provide a long-term depot for antigen in the course of virus infections [9], promoting T cell immunity. In the tumor

context, the role of LECs in regulating T cell responses is not as clear. In the B16F10 melanoma model, tumor-associated and draining LN LECs have been found to present tumor antigen on MHC-I [10], while forced induction of LEC expansion via overexpression of the lymphangiogenic growth factor VEGF-C in tumor cells had inconsistent effects on tumor immunity and the efficacy of experimental immunotherapeutic approaches, depending on the time point [10,11].

Another open question relates to the mechanism of LEC-mediated T cell inhibition (or activation). Under steady-state conditions, LN LECs generally do not express co-stimulatory molecules, but instead express high levels of T cell co-inhibitory molecules, including PD-L1 [6]. Systemic inhibition of the PD-L1 / PD-1 axis facilitated autoimmune $CD8^+$ responses against the LEC-expressed self-antigen tyrosinase, demonstrating that PD-L1 is involved in LEC-mediated peripheral tolerance [6]. However, the precise involvement of PD-L1 expressed by LECs themselves has not been elucidated. Similarly, in tumor immunity, we and others have shown that tumor-associated LECs upregulate PD-L1 expression in mouse tumor models, most likely in response to IFNγ produced in the tumor microenvironment [12,13], and chimeric mice lacking stromal PD-L1 expression showed increased $CD8^+$ T cell activation and a better response towards adoptive T cell therapy (ACT) in the B16F10 model expressing ovalbumin as model antigen (B16-ova) [13]. However, multiple stromal cell types in the tumor microenvironment or the draining LNs may express PD-L1 and contribute to T cell regulation in this case, so the precise function of LEC-expressed PD-L1 in tumor immunity has remained unknown. To clarify this question, we have generated a lymphatic-specific PD-L1 knockout mouse model and have investigated $CD8^+$ T cell responses in two independent syngeneic tumor models as well as in ACT in detail.

MATERIAL AND METHODS

Mice

$PD\text{-}L1^{flox}$ mice [14] were obtained from Lexicon / Taconic and backcrossed to the C57BL/6 background by speed congenics before crossing them with Prox1-Cre-ER^{T2} mice ([15], kindly provided by Dr. Taija Mäkinen, Uppsala University, Sweden) to create $PD\text{-}L1^{LECKO}$ mice. To induce Cre-mediated

recombination, these mice were treated with 50 mg/kg tamoxifen (Sigma) in sunflower oil for 5 days by intraperitoneal injection. 3-4 days after the last injection, mice were inoculated with tumor cells as described below. Cre-negative, PD-L1$^{fl/fl}$ littermates served as controls and were equally treated with tamoxifen. Ly5.1^{+} OT-1 mice were kindly provided by Dr. Roman Spörri, ETH Zurich, Switzerland. All mice were bred and housed in an SOPF facility at ETH Zurich. All experimental procedures were approved by the responsible ethics committee (Kantonales Veterinäramt Zürich, license 5/18).

Generation of PD-L1 ko LECs and OT-1 priming in vitro

Immortalized mouse LECs [16] were maintained on dishes coated with 10 µg/ml fibronectin (Millipore) and 10 µg/ml collagen type-1 (Advanced Biomatrix) in DMEM/F12 medium (Gibco) supplemented with 20% FBS (Gibco), 56 µg/ml heparin (Sigma), 10 µg/ml EC growth supplement (BioRad) and 1 U/ml recombinant mouse IFNγ (Peprotech) at 33°C, 5% CO_2. Before experiments, IFNγ was removed, and cells were shifted to 37°C. To delete PD-L1 expression, the CrispR-Cas9n double nickase approach was used essentially as described before [17]. In brief, a pair of sgRNAs were designed for a target sequence in exon 3 of the mouse CD274 (coding for PD-L1) gene using the online tool at http://crispr.mit.edu and were cloned into pSpCas9n(BB)-2A-GFP (Addgene, #48140). LECs were transfected with the vectors using polyethylenimine as described [18]. 24 h later, successfully transfected GFP^{+} cells were isolated using a FACS ARIA II instrument (BD) and expanded in culture. Cells with successful PD-L1 deletion were isolated by two rounds of FACS sorting after O/N stimulation with 100 ng/ml IFNγ and staining with PD-L1-PE/Cy7 (clone 10F.9G2, Biolegend 124314, 1:200). Cells retaining PD-L1 expression were isolated simultaneously and served as controls.

Priming experiments were performed essentially as described before [12]. 10,000 PD-L1^{-} and PD-L1^{+} LECs were seeded in coated 96-well plates and cultured O/N (in quintuplicates). The following day, cells were pulsed with 1 ng/ml SIINFEKL peptide (AnaSpec) for 30 min, washed twice with PBS, and subsequently co-cultured O/N with 100,000 CD8^{+} T cells freshly isolated from spleens of naïve Ly5.1^{+} OT-1 mice by positive MACS separation (Miltenyi) in T cell medium (RPMI supplemented

with 10% FBS, pyruvate, non-essential amino acids, 10 mM HEPES (all from Gibco) and 50 µM β-ME (Sigma)). Subsequently, cells were stained with Zombie-Aqua (Biolegend 423102, 1:500), CD8-FITC (clone 53-6.7, Biolegend 100706, 1:200), CD69-APC/Cy7 (clone H1.2F3, Biolegend 104526, 1:200), PD1-APC (clone RMP1-30, Biolegend 109112, 1:200), PD-L1-PE (clone MIH5, eBioscience 12-5982-82, 1:200), Ki67-eFluor450 (clone SolA15, eBioscience 48-5698-82, 1:200) and IFNγ-PE/Cy7 (clone XMG1.2, Biolegend 505826, 1:200) using an intracellular staining kit (eBioscience) according to the manufacturer's instructions, and analyzed using a Cytoflex S instrument (Beckman Coulter). Data were analyzed using FlowJo v10.5.3 (BD).

Tumor models

To generate MC38 cells expressing chicken ovalbumin (MC38-ova), we cloned the full-length ovalbumin coding sequence (Addgene, #64599) into a modified lentiviral vector in which the transgene is driven by a pgk-promoter and followed by an internal ribosomal entry site and an eGFP sequence [19]. Lentiviral particles were generated in HEK293T cells (kindly provided by Dr. Laure-Anne Ligeon, University of Zurich) using a 3rd generation packaging system. 48 h after transformation, single GFP^+ MC38 colorectal carcinoma cells (kindly provided by Dr. Tiziana Schioppa, Humanitas Clinical and Research Center, Milan, Italy) were sorted into 96-well plates and expanded in DMEM (Gibco) with 10% FBS at 37°C, 5% CO_2. A clone with high GFP expression but identical growth kinetics to the parental MC38 cells (data not shown) was selected for all further experiments. For orthotopic tumor growth, 200,000 MC38-ova cells in 20 µl PBS were injected into the rectal mucosa, and tumors were allowed to grow for 21 days until sacrifice.
B16F10 cells expressing ovalbumin (B16-ova, [12]) were cultured in DMEM supplemented with 10% FBS and 1.5 mg/ml G418 (Roche). 200,000 tumor cells in 20 µl PBS were injected intradermally into the shaved flank skin and tumor growth was monitored by caliper measurements until the study endpoint. All tumor cells were routinely checked for mycoplasma contamination.

Adoptive T cell therapy

OT-1 effector T cells were generated by ex vivo culture of total Ly5.1$^+$ OT-1 splenocytes in T cell medium supplemented with 1 ng/ml SIINFEKL peptide and 100 U/ml recombinant mouse IL-2 (ImmunoTools) for 72 h. 1x10^6 OT-1 effector T cells in 100 µl unsupplemented RPMI were transferred by tail vein injection on day 10 after tumor cell inoculation.

Flow cytometry

LN stromal cells were isolated and enriched as described before [20]. The non-stromal fractions obtained after pre-digestion were pooled with one third of the stromal-enriched fraction and used for LN T cell analyses. Tumors were digested in 3.5 mg/ml collagenase type IV (Gibco) in DMEM with 2% FBS and 1.2 mM $CaCl_2$ for 30 min at 37°C and passed through a cell strainer, before erythrocyte lysis using PharmLyse buffer (BD). Spleens were dissociated mechanically over a cell strainer and erythrocyte lysis was performed. Cell suspensions were resuspended in FACS buffer (PBS, 1% FBS, 1 mM EDTA, 0.02% NaN3) and treated with anti-CD16/CD32 (clone 93, Biolegend 101302, 1:100) for 20 min on ice before staining.

To determine PD-L1 expression in LN stromal cells, the remaining stromal-enriched fractions were stained with CD31-FITC (clone MEC13.3, BD, 553372, 1:300), podoplanin-PE (clone 8.1.1, eBioscience 12-5381-82, 1:400), CD45-PerCP (clone 30-F11, BD 557235, 1:100), PD-L1-APC (clone 10F.9G2, Biolegend 124312, 1:200) or PD-L1-PE/Cy7 (clone 10F.9G2, Biolegend 124314, 1:200), and Zombie-NIR (Biolegend 423106, 1:500) or Zombie-Aqua and were analyzed on a FACS ARIA II or a FACS Fortessa instrument (both BD). T cell and DC responses were examined using Zombie-Aqua, Apotracker-Green (Biolegend 427401, 1:200), CD45-PacificBlue (clone 30-F11, Biolegend 103126, 1:400), CD3-PE/Cy7 (clone 145-2C11, Biolegend 100320, 1:400), CD8-FITC (1:400) or CD8-APC/Cy7 (clone 53-6.7, Biolegend 100714, 1:400), CD4-PerCp (clone GK1.5, Biolegend 100432, 1:100), CD25-BV605 (clone PC61, Biolegend 102035, 1:400), CD69-APC/Cy7 (1:400), PD1-APC (1:200), CD44-BV650 (clone IM7, Biolegend 103049, 1:800), CD62L-Alexa700 (clone MEL-14, Biolegend 104426, 1:400), CD11c-PE/Cy7 (clone N418, Biolegend 117318, 1:400), MHC-II-Alexa700 (clone M5/114.15.2, Biolegend 107622, 1:800), CD80-FITC (clone 16-10A1, eBioscience 11-0801-85, 1:400), CD86-PE (clone GL1, eBioscience 12-0862-85, 1:400) and PE-

conjugated tetramers (control: H-2K^b-SIYRYYGL, ova: H-2K^b-SIINFEKL, pmel: H-2D^b-EGSRNQDWL, all NIH tetramer core facility, 1:800), followed by intracellular staining with Foxp3-PE/eFluor610 (clone FJK-16s, eBioscience 61-5773-82, 1:200) or Ki67-eFluor450 and analysis on a 4 laser Cytoflex S instrument (Beckmann Coulter). Data were analyzed using FlowJo v10.5.3 (BD).

Statistical analysis

Statistical analysis was done using GraphPad Prism. Graphs show mean values ± standard deviation. Number of replicates and test details are indicated in the corresponding figure legends.

RESULTS

Lymphatic PD-L1 impairs T cell priming by lymphatic endothelial cells in vitro

We previously reported that antibody-mediated blockade of PD-L1 promoted the priming of naïve CD8$^+$ OT-1 cells by SIINFEKL-presenting cultured mouse LECs [12]. However, as PD-L1 is also expressed by CD8$^+$ OT-1 cells themselves and is induced upon activation, we could not rule out that antibody-mediated inhibition of endogenously expressed PD-L1 in CD8$^+$ OT-1 cells also contributed to this effect. To elucidate the function of PD-L1 expressed by antigen-presenting LECs specifically, we first generated PD-L1 deficient LECs using the CrispR-Cas9n approach in vitro. Cultured wildtype LECs expressed surface PD-L1 under steady-state conditions, and this expression was strongly inducible by IFNγ, whereas PD-L1 ko LECs had completely lost PD-L1 expression on their cell surface (Fig. 1A, 1B). When loaded with the SIINFEKL peptide, PD-L1 ko LECs were able to prime naïve OT-1 cells more efficiently than wildtype LECs, resulting in increased expression of CD69, IFNγ, and a higher proliferation rate indicated by Ki67 expression (Fig. 1C-E). Additionally, PD-L1 and PD-1 expression were increased in OT-1 cells primed by PD-L1 ko LECs compared to wildtype LECs, most likely as part of an activation-induced negative feedback mechanism limiting an even stronger T cell response (Fig. 1F, 1G). Together, these data demonstrate that PD-L1 expression by antigen-presenting LECs impairs priming of naïve CD8$^+$ T cells in vitro.

Generation of a conditional, lymphatic-specific PD-L1 knockout mouse model

PD-L1 is constitutively expressed by LN LECs [6] and is induced in tumor-associated lymphatic vessels in several tumor models, including the B16F10 melanoma model [12,13]. We generated a conditional, lymphatic-specific PD-L1 ko mouse model ("PD-L1^{LECKO} mice") by crossing PD-L1^{flox} mice [14] with the Prox1-Cre-ER^{T2} line [15] (Fig. 2A). As expected, PD-L1 was robustly expressed in LN LECs in naïve PD-L1^{LECKO} mice, and was efficiently deleted upon tamoxifen treatment (Fig. 2B, 2C). In contrast, Prox1-negative LN blood vascular endothelial cells (BECs) showed a lower baseline expression of PD-L1, and this expression was not affected by tamoxifen (Fig. 2D, 2E). Thus, PD-L1^{LECKO} mice are a suitable model to elucidate the effect of lymphatic PD-L1 on endogenously generated immune responses in vivo.

Lymphatic PD-L1 deletion amplifies tumor-specific CD8$^+$ T cell responses

In order to elucidate the role of LEC-expressed PD-L1 in tumor-specific CD8$^+$ T cell responses, we first treated PD-L1^{LECKO} mice with tamoxifen, and subsequently implanted B16-ova melanoma cells orthotopically into the flank skin. Cre-negative littermate mice served as controls. Primary tumor growth was not affected by lymphatic PD-L1 deletion (Fig. 3A). This is in agreement with a previous report showing that growth of B16-ova tumors was not affected in bone marrow-chimeric mice lacking stromal PD-L1 expression [13]. In contrast to this report however, we did not observe an increase in the frequency of CD8$^+$ T cells, neither in the primary tumor, nor in draining LNs or the spleen (Fig. 3B), suggesting that PD-L1 expression on stromal cells other than LECs controls overall accumulation of CD8$^+$ T cells in the tumor tissue. Next, we used flow cytometry to analyze the T cell response at the study endpoint in greater detail (Supplementary Fig. S1). Importantly, using tetramers to detect CD8$^+$ T cells specific for the SIINFEKL peptide derived from the model antigen ovalbumin and the EGSRNQDWL peptide derived from the endogenous melanoma antigen pmel/gp100 which is expressed by B16F10 cells [21], we found a significant increase in the frequency of these cells in the draining LNs (both ova- and pmel-specific T cells) and the spleen (only pmel-specific T cells), but not in the primary tumors (Fig. 3C-E). No changes in the activation profile or the memory status of the overall CD8$^+$ T cell population could be detected, while the frequency of CD4$^+$ FoxP3$^+$ T_{reg} cells was

slightly reduced in the spleen of Cre-positive PD-L1^{LECKO} mice (Supplementary Fig. S2A-C). These data indicate that lymphatic PD-L1 limits priming, expansion or survival of tumor-specific CD8$^+$ T cells in vivo, particularly in tumor-draining LNs where lymphatic PD-L1 expression is constitutively high.

We sought to validate our findings in a second, independent tumor model. To this end, we engineered MC38 colorectal carcinoma cells to express ovalbumin and implanted them orthotopically into the rectal mucosa of PD-L1^{LECKO} mice and Cre-negative control littermates. Three weeks later, tumors, draining (caudal mesenteric and iliac) LNs and spleens were collected and analyzed. Notably, like in the B16F10 model [12,13], tumor-associated lymphatic vessels strongly upregulated PD-L1 expression (Fig. 3F). Tumor weight at the endpoint was not significantly affected by lymphatic PD-L1 deletion, although we observed a trend towards smaller tumors in PD-L1^{LECKO} mice (Fig. 3G). Importantly, while the overall frequency of CD8$^+$ T cells was not changed as in the B16-ova model (Fig. 3H), the frequency of tumor (ova)-specific CD8$^+$ T cells was again increased in tumor-draining LNs, but not in the primary tumor or the spleen (Fig. 3I-K). Likewise, we found no major differences in the activation profile and the memory status of the total CD8$^+$ T cell population in any of the organs analyzed (Supplementary Fig. S2D, S2E). Thus, lymphatic PD-L1 expression impairs the expansion of tumor-specific T cells independently of the tumor model and the site of tumor cell injection.

In addition to its role in T cell regulation, lymphatic PD-L1 has also been suggested to have a LN LEC-intrinsic function, regulating LEC expansion and contraction in the course of inflammatory responses [22]. However, in our hands, deletion of PD-L1 in LECs had no effect on the LEC frequency in LNs in tumor-bearing mice (Supplementary Fig. S3).

Deletion of lymphatic PD-L1 increases the efficiency of adoptive T cell therapy

Complete stromal knockout of PD-L1 has previously been reported to augment the anti-tumor effect of adoptive T cell therapy (ACT) with pre-activated OT-1 cells in the B16-ova model [13]. To test if this effect was due to PD-L1 expression by LECs or by other stromal cells, we injected B16-ova cells in

the flank skin and subsequently treated the mice with pre-activated effector OT-1 cells on day 10 after tumor inoculation via the tail vein (Fig. 4A). The tumor weight at the endpoint (day 17) was clearly reduced in PD-L1^{LECKO} mice compared to Cre-negative control littermates (Fig. 4B), demonstrating that deletion of lymphatic PD-L1 augments the efficiency of ACT. We also performed the same therapeutic approach in MC38-ova bearing mice, but in this case, tumors were completely eradicated by the transfer of OT-1 cells, irrespective of lymphatic PD-L1 expression, preventing us from drawing further conclusions (data not shown). Flow cytometry revealed a significantly improved infiltration of CD8$^+$ T cells into B16-ova tumors in ACT-treated PD-L1^{LECKO} mice (Fig. 4C). In addition, we again noted an increased frequency of endogenous SIINFEKL-specific CD8$^+$ cells in PD-L1^{LECKO} mice, which was statistically significant in tumor-draining LNs (Fig. 4D-F). On the other hand, no changes in the frequency of transferred OT-1 cells could be detected (Fig. 4G), and their activation and memory profile were also equal between the two groups (data not shown). Thus, these data indicate that lymphatic PD-L1 primarily effects endogenously generated CD8$^+$ T cell responses, which in cooperation with transferred exogenous effector cells can reduce tumor growth.

Lymphatic PD-L1 does not affect DC activation

APCs, including DCs and macrophages, have been shown to express PD-1 [23,24], and may receive inhibitory signals from PD-L1 expressing LECs as they migrate from the tumor microenvironment to draining LNs. Thus, lymphatic PD-L1 may affect endogenous T cell activation indirectly via regulation of DC activation. To investigate this further, we analyzed the phenotype of both migratory (CD11^{int} MHC-II^{hi}) and resident (CD11c^{hi} MHC-II^{int}) DCs in tumor-draining LNs. However, PD-1 expression in DCs in draining LNs was very low in our hands, and the expression level of the co-stimulatory molecules CD80 and CD86 were not affected by lymphatic PD-L1 deletion (Supplementary Fig. S4).

Lymphatic PD-L1 regulates apoptosis in tumor-specific CD8$^+$ central memory cells

Since LEC-expressed PD-L1 had no influence on the phenotype of DCs in tumor-draining LNs, we wondered whether PD-L1-expressing LN LECs might directly restrain tumor-specific T cells.

Previously, it has been suggested that LECs induce apoptosis of $CD8^+$ T cells in vitro [7]. Thus, we hypothesized that the increase in tumor-specific $CD8^+$ T cells in PD-L1LECKO mice might be due to reduced apoptosis. Indeed, FACS-based analysis revealed that the apoptosis of both ova- and pmel-specific $CD8^+$ T cells in B16-ova-draining LNs was significantly reduced after deletion of lymphatic PD-L1 (Fig. 5A), while the proliferation rate (assessed by Ki67 expression) was not affected (Supplementary Fig. S5A). Surprisingly, further analysis of the rate of apoptosis in ova- and pmel-specific $CD44^+$ $CD62L^-$ effector memory (EM), $CD44^+$ $CD62L^+$ central memory (CM) and $CD44^-$ $CD62L^-$ naïve $CD8^+$ T cells revealed that lymphatic PD-L1 primarily affects cells with a CM phenotype. In addition, apoptosis of naïve tumor-specific T cells was also reduced, although these cells have a generally low level of apoptosis (Fig. 5B, 5C). In line with this, we noted a selective expansion of ova-specific CM cells in B16-ova-draining LNs (Supplementary Fig. S5B), which however did not reach statistical significance ($p = 0.072$). Similar findings were made in the MC38-ova tumor model. Although the rate of apoptosis of all ova-specific $CD8^+$ T cells was not significantly altered in this case (Fig 5D), ova-specific CM cells again showed reduced apoptosis in PD-$L1^{LECKO}$ mice compared to control littermates (Fig. 5E). Thus, lymphatic PD-L1 limits tumor immunity predominantly by inducing apoptosis in tumor-specific $CD8^+$ CM T cells in tumor-draining LNs, most likely via direct interactions between T cells and LECs.

DISCUSSION

Although PD-L1 is a well-known T cell checkpoint molecule and immunotherapeutic approaches targeting it or its receptor PD-1 have been impressively successful in a subset of patients suffering from several cancer types, the precise modalities and characteristics of its inhibitory effects on the immune system, for instance with regards to the different phase of a typical T cell response such as priming, expansion, exhaustion, constriction and memory formation, are still not well understood [25]. Furthermore, since PD-L1 may be expressed or induced both in tumor cells as well as in various host-derived cell types, including hematopoietic and stromal cell populations, the most relevant sites and cell types involved in PD-L1 action during tumor immunity are still controversial. For example, contradictory results have been published regarding the role of PD-L1 expressed by tumor cells as

compared to host-derived cells in several tumor models in mice, including the B16F10 and the MC38 models used here. While some studies indicate that PD-L1 expression by tumor cells is sufficient to impair tumor immunity, most studies currently conclude that host PD-L1 is critically important [26-29]. In line with this, it is becoming increasingly clear that PD-L1 expression by tumor cells alone is no reliable predictor of patient responsiveness to PD-1 or PD-L1 targeting therapies [30], further suggesting that PD-L1 expression by either hematopoietic or stromal host cell types may be equally (or even more) relevant for tumor immunity and immunotherapy outcomes.

A recent study by Lane et al., using bone marrow chimeric mice, demonstrated that PD-L1 in both hematopoietic and radio-resistant (stromal) cells affected T cell immune responses in the B16F10 melanoma model [13]. Yet, it remained unclear which stromal cell types were involved. Our data reveal that PD-L1 expressed by LECs contributes to tumor immune evasion, via a distinctive mechanism affecting primarily tumor-specific $CD8^+$ CM T cells. Deletion of lymphatic PD-L1 reduced apoptosis of these cells and allowed for a general expansion of tumor-specific $CD8^+$ T cells in tumor-draining LNs, where PD-L1 expression by LECs is highest. This was not sufficient though to elicit a strong T cell infiltration into the primary tumor and consequently had no major effect on primary tumor growth, at least in the B16F10 model which is poorly immunogenic and inherently resistant to therapies targeting the PD-L1 / PD-1 axis [31-34]. In contrast, complete stromal PD-L1 deletion had broader effects on the $CD8^+$ T cell response in B16F10-bearing mice, including an overall increased accumulation of $CD8^+$ T cells in the primary tumor, most likely due to PD-L1 expression in stromal cells other than LECs [13]. Nonetheless, our data may explain why some cancer patients without measurable PD-L1 expression in the tumor microenvironment still respond very well to PD-1 / PD-L1 targeting therapies. Consequently, assessment of PD-L1 expression in tumor-associated and, maybe more importantly, draining LN residing LECs might be useful as an additional predictive biomarker to select patients for this kind of therapy.

PD-L1 expression is induced in primary tumor-associated LECs [12,13], which conceivably leads to inhibition or deletion of PD-1^+ EM and CM T cells that have the capacity to recirculate from the tumor microenvironment to tumor-draining LNs via the lymphatic system [35]. Additionally, PD-L1

expression is constitutively high in LN LECs [6], both in cells lining the floor of the subcapsular sinus and the medullary sinuses [5,36]. PD-L1 expressed by both subcapsular sinus and medullary sinus LECs could equally affect T cells recirculating from upstream tissues and entering the LN via afferent lymphatics [37,38]. Additionally, medullary LEC-expressed PD-L1 could interact with PD-1$^+$ T cells exiting the LN via efferent lymphatics. This would apply to CM T cells that previously entered the LN via the blood circulation, but could also include freshly primed T cells, which have been shown to rapidly upregulate PD-1 and to be sensitive to PD-L1 / PD-1 inhibition [39]. Our data do not allow us to determine precisely whether the T cells affected by lymphatic PD-L1 expression were derived from the tumor microenvironment or entered the draining LNs via the blood stream. Nonetheless, they clearly demonstrate lymphatic PD-L1 primarily acts on T cells with a classic CM phenotype (CD44$^+$ CD62L$^+$), whereas EM and naïve T cells in draining LNs were not or only marginally affected by it. This is somewhat surprising, given that EM T cells are highly enriched among tumor-derived recirculating T cells [35] and expressed the highest level of PD-1, followed by CM cells with intermediate PD-1 expression and naïve T cells that were essentially PD-1$^-$ (data not shown). Possibly, tumor-derived EM T cells were already in a dysfunctional state of activation due to their journey through the tumor microenvironment, and thus were not sensitive to additional inhibitory signals via lymphatic PD-L1.

The primary effect of lymphatic PD-L1 deletion on tumor-specific CM cells was reduced apoptosis induction, while proliferation (and activation, data not shown) were not significantly affected. This was surprising given that PD-1 stimulation on T cells impairs activating signals from the T cell receptor and CD28, and is generally believed to primarily inhibit T cell proliferation and effector functions (reviewed in [40,41]). However, PD-1 signaling also impairs the PI3K-Akt pathway known to be involved in cell survival, and has been shown to impair expression of the anti-apoptotic protein Bcl-x_L [42]. Congruently, PD-L1 expression by tumor cells induced effector T cell apoptosis in vitro and in vivo, although this effect was suggested not to be mediated by PD-1 [43], indicating that CD80, another receptor for PD-L1 [44], may be involved. Furthermore, ova-presenting LECs upregulated PD-L1 when cultured together with naïve OT-1 T cells and induced their apoptosis during priming [7].

Together, these and our data suggest that LECs have the capacity to induce apoptosis of both freshly primed and memory T cells via PD-L1.

In conclusion, our data reveal that LECs contribute to tumor immune evasion via PD-L1-mediated apoptosis induction in tumor-specific $CD8^+$ CM T cells, and warrant further studies to investigate the predictive value of lymphatic PD-L1 expression for cancer immunotherapy.

ACKNOWLEDGEMENT

The authors would like to thank Jeannette Scholl (ETH Zurich) for technical support, and Dr. Roman Spörri (ETH Zurich) and the NIH tetramer core facility for provision of vital reagents. This work was supported by ERC grant LYVICAM and Swiss National Science Foundation grants 310030_166490 and 310030B_185392 (to M.D.), and a career seed grant by ETH Zurich and research grants from the Vontobel Foundation and Krebsliga Zurich (to L.C.D.). The authors have no conflicting financial interests.

AUTHOR CONTRIBUTIONS

Conceptualization and study design: M.D. and L.C.D.; Experimental work: S.C., M.Di., N.C., C.T. and L.C.D.; Data analysis and interpretation: S.C., M.Di., L.C.D.; Manuscript writing: M.D. and L.C.D.

COMPETING INTERESTS

None declared.

REFERENCES

1 Ma, Q., Dieterich, L. C. & Detmar, M. Multiple roles of lymphatic vessels in tumor progression. *Curr. Opin. Immunol.* **53**, 7-12, doi:10.1016/j.coi.2018.03.018 (2018).

2 Maisel, K., Sasso, M. S., Potin, L. & Swartz, M. A. Exploiting lymphatic vessels for immunomodulation: Rationale, opportunities, and challenges. *Adv. Drug Deliv. Rev.* **114**, 43-59, doi:10.1016/j.addr.2017.07.005 (2017).

3 Cohen, J. N. *et al.* Lymph node-resident lymphatic endothelial cells mediate peripheral tolerance via Aire-independent direct antigen presentation. *J. Exp. Med.* **207**, 681-688, doi:10.1084/jem.20092465 (2010).

4 Fletcher, A. L. *et al.* Lymph node fibroblastic reticular cells directly present peripheral tissue antigen under steady-state and inflammatory conditions. *J. Exp. Med.* **207**, 689-697, doi:10.1084/jem.20092642 (2010).

5 Cohen, J. N. *et al.* Tolerogenic properties of lymphatic endothelial cells are controlled by the lymph node microenvironment. *PLoS One* **9**, e87740, doi:10.1371/journal.pone.0087740 (2014).

6 Tewalt, E. F. *et al.* Lymphatic endothelial cells induce tolerance via PD-L1 and lack of costimulation leading to high-level PD-1 expression on CD8 T cells. *Blood* **120**, 4772-4782, doi:10.1182/blood-2012-04-427013 (2012).

7 Hirosue, S. *et al.* Steady-state antigen scavenging, cross-presentation, and CD8+ T cell priming: a new role for lymphatic endothelial cells. *J. Immunol.* **192**, 5002-5011, doi:10.4049/jimmunol.1302492 (2014).

8 Vokali, E. *et al.* Lymphatic endothelial cells prime naive CD8(+) T cells into memory cells under steady-state conditions. *Nat. Commun.* **11**, 538, doi:10.1038/s41467-019-14127-9 (2020).

9 Tamburini, B. A., Burchill, M. A. & Kedl, R. M. Antigen capture and archiving by lymphatic endothelial cells following vaccination or viral infection. *Nat. Commun.* **5**, 3989, doi:10.1038/ncomms4989 (2014).

10 Lund, A. W. *et al.* VEGF-C promotes immune tolerance in B16 melanomas and cross-presentation of tumor antigen by lymph node lymphatics. *Cell Rep.* **1**, 191-199, doi:10.1016/j.celrep.2012.01.005 (2012).

11 Fankhauser, M. *et al.* Tumor lymphangiogenesis promotes T cell infiltration and potentiates immunotherapy in melanoma. *Sci. Transl. Med.* **9**, doi:10.1126/scitranslmed.aal4712 (2017).

12 Dieterich, L. C. *et al.* Tumor-Associated Lymphatic Vessels Upregulate PDL1 to Inhibit T-Cell Activation. *Front. Immunol.* **8**, 66, doi:10.3389/fimmu.2017.00066 (2017).

13 Lane, R. S. *et al.* IFNgamma-activated dermal lymphatic vessels inhibit cytotoxic T cells in melanoma and inflamed skin. *J. Exp. Med.* **215**, 3057-3074, doi:10.1084/jem.20180654 (2018).

14 Carter, L. L. *et al.* PD-1/PD-L1, but not PD-1/PD-L2, interactions regulate the severity of experimental autoimmune encephalomyelitis. *J. Neuroimmunol.* **182**, 124-134, doi:10.1016/j.jneuroim.2006.10.006 (2007).

15 Bazigou, E. *et al.* Genes regulating lymphangiogenesis control venous valve formation and maintenance in mice. *J. Clin. Invest.* **121**, 2984-2992, doi:10.1172/JCI58050 (2011).

16 Vigl, B. *et al.* Tissue inflammation modulates gene expression of lymphatic endothelial cells and dendritic cell migration in a stimulus-dependent manner. *Blood* **118**, 205-215, doi:10.1182/blood-2010-12-326447 (2011).

17 Ran, F. A. *et al.* Genome engineering using the CRISPR-Cas9 system. *Nat. Protoc.* **8**, 2281-2308, doi:10.1038/nprot.2013.143 (2013).

18 Hsu, C. Y. & Uludag, H. A simple and rapid nonviral approach to efficiently transfect primary tissue-derived cells using polyethylenimine. *Nat. Protoc.* **7**, 935-945, doi:10.1038/nprot.2012.038 (2012).

19 Dieterich, L. C. *et al.* alphaB-crystallin/HspB5 regulates endothelial-leukocyte interactions by enhancing NF-kappaB-induced up-regulation of adhesion molecules ICAM-1, VCAM-1 and E-selectin. *Angiogenesis* **16**, 975-983, doi:10.1007/s10456-013-9367-4 (2013).

20 Commerford, C. D. *et al.* Mechanisms of Tumor-Induced Lymphovascular Niche Formation in Draining Lymph Nodes. *Cell Rep.* **25**, 3554-3563 e3554, doi:10.1016/j.celrep.2018.12.002 (2018).

21 Tsukamoto, K., Hirata, S., Osada, A., Kitamura, R. & Shimada, S. Detection of circulating melanoma cells by RT-PCR amplification of three different melanocyte-specific mRNAs in a

mouse model. *Pigment Cell Res.* **13**, 185-189, doi:10.1034/j.1600-0749.2000.130311.x (2000).

22 Lucas, E. D. *et al.* Type 1 IFN and PD-L1 Coordinate Lymphatic Endothelial Cell Expansion and Contraction during an Inflammatory Immune Response. *J. Immunol.* **201**, 1735-1747, doi:10.4049/jimmunol.1800271 (2018).

23 Gordon, S. R. *et al.* PD-1 expression by tumour-associated macrophages inhibits phagocytosis and tumour immunity. *Nature* **545**, 495-499, doi:10.1038/nature22396 (2017).

24 Strauss, L. *et al.* Targeted deletion of PD-1 in myeloid cells induces antitumor immunity. *Sci. Immunol.* **5**, doi:10.1126/sciimmunol.aay1863 (2020).

25 Sharpe, A. H. & Pauken, K. E. The diverse functions of the PD1 inhibitory pathway. *Nat. Rev. Immunol.* **18**, 153-167, doi:10.1038/nri.2017.108 (2018).

26 Juneja, V. R. *et al.* PD-L1 on tumor cells is sufficient for immune evasion in immunogenic tumors and inhibits CD8 T cell cytotoxicity. *J. Exp. Med.* **214**, 895-904, doi:10.1084/jem.20160801 (2017).

27 Lau, J. *et al.* Tumour and host cell PD-L1 is required to mediate suppression of anti-tumour immunity in mice. *Nat. Commun.* **8**, 14572, doi:10.1038/ncomms14572 (2017).

28 Lin, H. *et al.* Host expression of PD-L1 determines efficacy of PD-L1 pathway blockade-mediated tumor regression. *J. Clin. Invest.* **128**, 805-815, doi:10.1172/JCI96113 (2018).

29 Tang, H. *et al.* PD-L1 on host cells is essential for PD-L1 blockade-mediated tumor regression. *J. Clin. Invest.* **128**, 580-588, doi:10.1172/JCI96061 (2018).

30 Havel, J. J., Chowell, D. & Chan, T. A. The evolving landscape of biomarkers for checkpoint inhibitor immunotherapy. *Nat. Rev. Cancer* **19**, 133-150, doi:10.1038/s41568-019-0116-x (2019).

31 Huang, L. *et al.* Mild photothermal therapy potentiates anti-PD-L1 treatment for immunologically cold tumors via an all-in-one and all-in-control strategy. *Nat. Commun.* **10**, 4871, doi:10.1038/s41467-019-12771-9 (2019).

32 Sanchez-Paulete, A. R. *et al.* Cancer Immunotherapy with Immunomodulatory Anti-CD137 and Anti-PD-1 Monoclonal Antibodies Requires BATF3-Dependent Dendritic Cells. *Cancer Discov.* **6**, 71-79, doi:10.1158/2159-8290.CD-15-0510 (2016).

33 Yu, J. W. *et al.* Tumor-immune profiling of murine syngeneic tumor models as a framework to guide mechanistic studies and predict therapy response in distinct tumor microenvironments. *PLoS One* **13**, e0206223, doi:10.1371/journal.pone.0206223 (2018).

34 Zhou, Z. *et al.* Perfluorocarbon nanoparticle-mediated platelet inhibition promotes intratumoral infiltration of T cells and boosts immunotherapy. *Proc. Natl. Acad. Sci. U. S. A.* **116**, 11972-11977, doi:10.1073/pnas.1901987116 (2019).

35 Torcellan, T. *et al.* In vivo photolabeling of tumor-infiltrating cells reveals highly regulated egress of T-cell subsets from tumors. *Proc. Natl. Acad. Sci. U. S. A.* **114**, 5677-5682, doi:10.1073/pnas.1618446114 (2017).

36 Fujimoto, N. *et al.* Single-cell mapping reveals new markers and functions of lymphatic endothelial cells in lymph nodes. *PLoS Biol.* **18**, e3000704, doi:10.1371/journal.pbio.3000704 (2020).

37 Braun, A. *et al.* Afferent lymph-derived T cells and DCs use different chemokine receptor CCR7-dependent routes for entry into the lymph node and intranodal migration. *Nat. Immunol.* **12**, 879-887, doi:10.1038/ni.2085 (2011).

38 Martens, R. *et al.* Efficient homing of T cells via afferent lymphatics requires mechanical arrest and integrin-supported chemokine guidance. *Nat. Commun.* **11**, 1114, doi:10.1038/s41467-020-14921-w (2020).

39 Ahn, E. *et al.* Role of PD-1 during effector CD8 T cell differentiation. *Proc. Natl. Acad. Sci. U. S. A.* **115**, 4749-4754, doi:10.1073/pnas.1718217115 (2018).

40 He, X. & Xu, C. Immune checkpoint signaling and cancer immunotherapy. *Cell Res.*, doi:10.1038/s41422-020-0343-4 (2020).

41 Boussiotis, V. A. Molecular and Biochemical Aspects of the PD-1 Checkpoint Pathway. *N. Engl. J. Med.* **375**, 1767-1778, doi:10.1056/NEJMra1514296 (2016).

42 Parry, R. V. *et al.* CTLA-4 and PD-1 receptors inhibit T-cell activation by distinct mechanisms. *Mol. Cell. Biol.* **25**, 9543-9553, doi:10.1128/MCB.25.21.9543-9553.2005 (2005).

43 Dong, H. *et al.* Tumor-associated B7-H1 promotes T-cell apoptosis: a potential mechanism of immune evasion. *Nat. Med.* **8**, 793-800, doi:10.1038/nm730 (2002).

44 Butte, M. J., Keir, M. E., Phamduy, T. B., Sharpe, A. H. & Freeman, G. J. Programmed death-1 ligand 1 interacts specifically with the B7-1 costimulatory molecule to inhibit T cell responses. *Immunity* **27**, 111-122, doi:10.1016/j.immuni.2007.05.016 (2007).

FIGURE LEGENDS

Figure 1. PD-L1 impairs CD8$^+$ T cell priming by LECs in vitro.

(A-B) Example histograms (A) and quantification (B) of PD-L1 expression in cultured mouse wildtype (WT) and PD-L1 ko LECs determined by FACS (N = 3 independent experiments). IFNγ (100 ng/ml) was used as positive control to further induce PD-L1 expression. (C-G) WT and PD-L1 ko LECs were loaded with SIINFEKL peptide (1 ng/ml) and co-cultured with freshly isolated CD8$^+$ OT-1 cells O/N. OT-1 expression of CD69 (C), IFNγ (D), Ki67 (E), PD-L1 (F) and PD-1 (G) were determined by FACS. Bar graphs show one representative of three independent experiments (N = 5 replicates). ** $p < 0.01$, **** $p < 0.0001$, one-way ANOVA with paired Sidak's post-test.

Figure 2. Validation of the lymphatic PD-L1 ko mouse model.

(A) Schematic representation of the lymphatic PD-L1 ko mouse model (PD-L1^{LECKO}). Prox1-Cre-ER^{T2} mice were crossed with PD-L1^{flox} mice and treated with tamoxifen for five days before initiation of tumor studies. (B-C) Representative FACS histogram (B) and quantification (C) of PD-L1 expression in LN LECs of Cre-positive PD-L1^{LECKO} mice and Cre-negative PD-L1^{flox} littermate controls. (D-E) Representative FACS histogram (D) and quantification (E) of PD-L1 expression in

LN BECs of Cre-positive PD-L1^{LECKO} mice and Cre-negative PD-L1^{flox} littermate controls (N = 3-4 mice/group). * $p < 0.05$, Student's t-test.

Figure 3. Lymphatic PD-L1 impairs tumor-specific CD8$^+$ T cell responses in mice bearing orthotopically implanted B16-ova melanomas and MC38-ova colorectal carcinomas.

(A) Growth curve of B16-ova cells in Cre-positive PD-L1^{LECKO} and Cre-negative littermate controls. Graph shows 1 representative of three independent experiments (N = 4-5 mice/group). (B) FACS-based quantification of CD8$^+$ T cells in tumor, draining LNs and spleen on day 16 after inoculation of B16-ova cells. The frequency of CD8$^+$ T cells is expressed as % of all living single cells. Graphs show pooled data from three independent experiments (N = 15 Cre-negative / 11 Cre-positive mice/group). (C-E) Quantification of CD8$^+$ T cells specific for ovalbumin (SIINFEKL peptide) or pmel/gp100 (EGSRNQDWL peptide) in tumors (C), draining LNs (D) and spleen (E) (N = 15 Cre-negative / 11 Cre-positive for ovalbumin; N = 8 for pmel). (F) Quantification of PD-L1 expression levels on LECs in normal colorectal mucosa (naïve) compared to LECs in orthotopically implanted MC38-ova tumors in Cre-negative control mice on day 21 after tumor cell inoculation (N = 3 mice/group). Graph represents the fluorescence intensity (FI) of PD-L1 compared to the corresponding isotype control. (G) Weight of orthotopically implanted MC38-ova tumors in Cre-positive PD-L1^{LECKO} mice and Cre-negative control littermates on day 21 after inoculation (N = 7 Cre-negative / 6 Cre-positive). (H) FACS-based quantification of CD8$^+$ T cells in tumor, draining LNs and spleen on day 21 after inoculation of MC38-ova cells. The frequency of CD8$^+$ T cells is expressed as % of all living single cells. (N = 4 Cre-negative / 6 Cre-positive mice/group in tumor; N = 7 Cre-negative / 6 Cre-positive in draining LN and spleen). (I-K) Quantification of CD8$^+$ T cells specific for ovalbumin (SIINFEKL peptide) in tumors (I), draining LNs (J) and spleen (K) (N = 4 Cre-negative / 6 Cre-positive mice/group in tumor; N = 7 Cre-negative / 6 Cre-positive in draining LN and spleen). * $p < 0.05$, Student's t-test.

Figure 4. Deletion of lymphatic PD-L1 increases the efficiency of adoptive T cell transfer in the B16-ova melanoma model.

(A) Schematic representation of adoptive T cell therapy (ACT) approach in mice bearing B16-ova tumors. $1x10^6$ OT-1 effector cells were intravenously transferred on day 10 after tumor cell inoculation, and tumors, draining LNs and spleens collected 1 week later for analysis. (B) Primary tumor weight in Cre-positive PD-L1^{LECKO} mice and Cre-negative littermate controls at the endpoint. (C) FACS-based quantification of $CD8^+$ T cells in tumor, draining LNs and spleen. The frequency of $CD8^+$ T cells is expressed as % of all living single cells. (D-F) Quantification of $CD8^+$ T cells specific for ovalbumin (SIINFEKL peptide) or pmel/gp100 (EGSRNQDWL peptide) in tumors (D), draining LNs (E) and spleen (F). (G) Frequency of endogenous and $CD45.1^+$ OT-1 $CD8^+$ T cells in tumors, draining LNs and spleens determined by FACS (N = 6 Cre-negative / 7 Cre-positive). * $p < 0.05$, Student's t-test.

Figure 5. Lymphatic PD-L1 induces apoptosis in tumor-specific $CD8^+$ central memory T cells in tumor-draining LNs.

(A-C) Frequency of apoptotic cells (both early ($Apotracker^+$ $Zombie^-$) and late ($Apotracker^+$ $Zombie^+$) apoptotic) among all ova- and pmel-specific $CD8^+$ T cells (A) or within $CD44^+CD62L^-$ effector memory (EM), $CD44^+CD62L^+$ central memory (CM) and $CD44^-CD62L^+$ naïve ova-specific (B) and pmel-specific (C) $CD8^+$ T cells in B16-ova-draining LNs assessed by FACS (N = 10 Cre-negative / 9 Cre-positive mice/group). (D-E) Frequency of apoptotic cells (both early ($Apotracker^+$ $Zombie^-$) and late ($Apotracker^+$ $Zombie^+$) apoptotic) among all ova-specific $CD8^+$ T cells (D) or within $CD44^+CD62L^-$ effector memory (EM), $CD44^+CD62L^+$ central memory (CM) and $CD44^-CD62L^+$ naïve ova-specific (C) $CD8^+$ T cells in MC38-ova-draining LNs (N = 5 mice/group). * $p < 0.05$, Student's t-test.

Figure 1

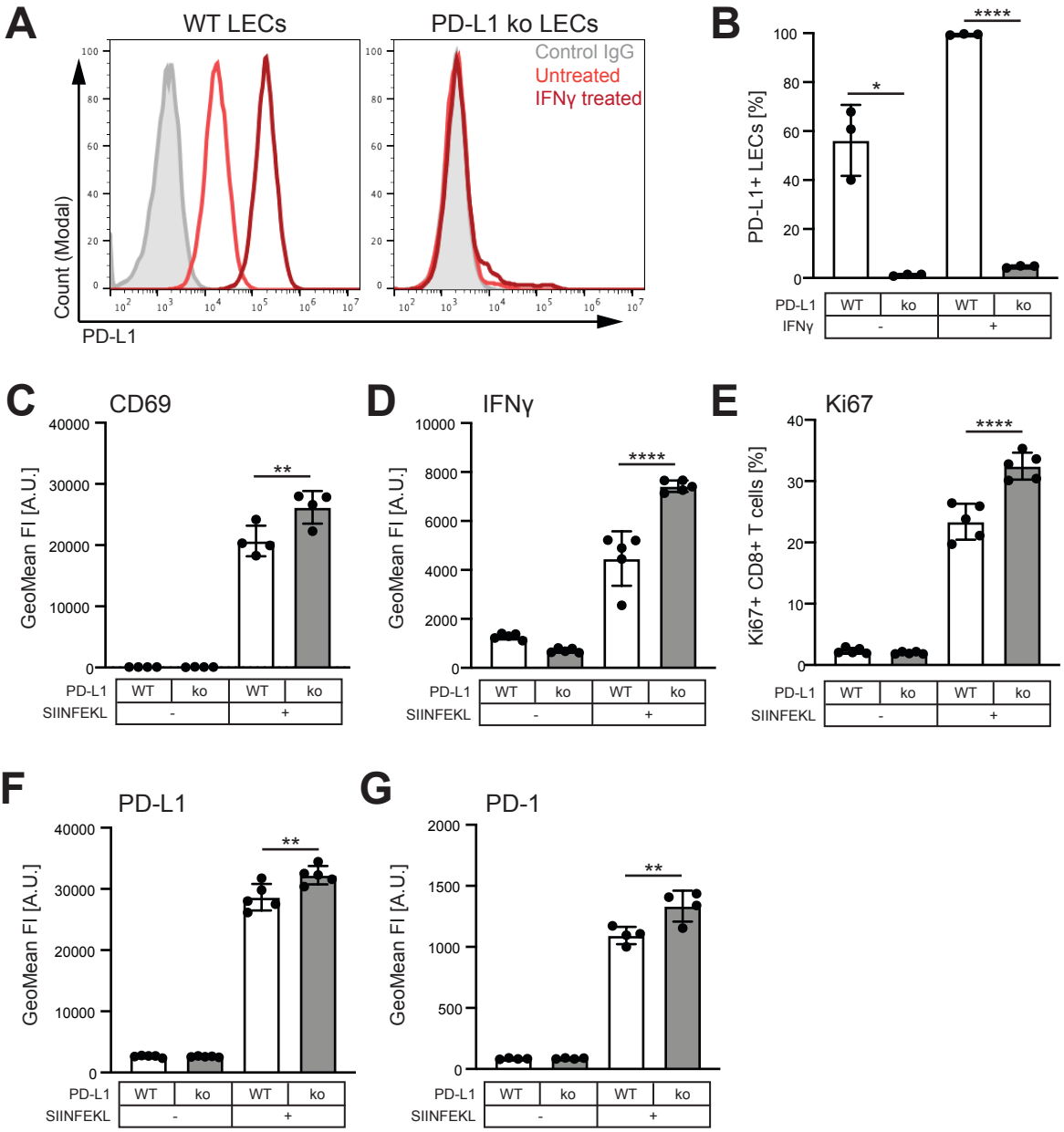

Figure 2

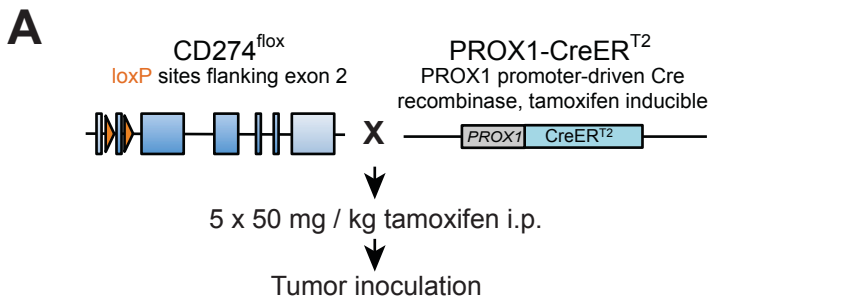

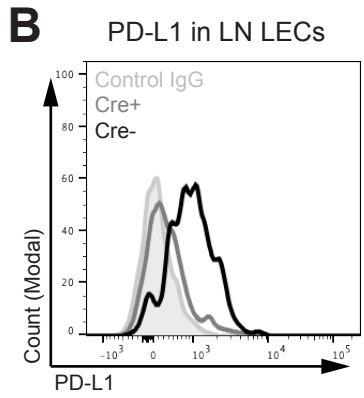

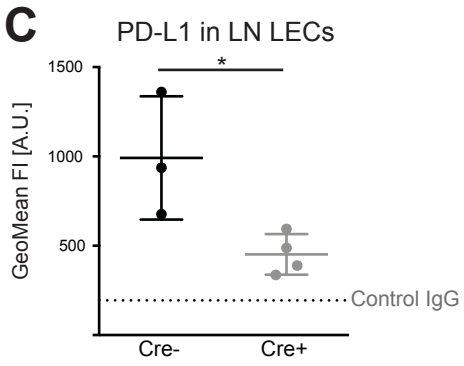

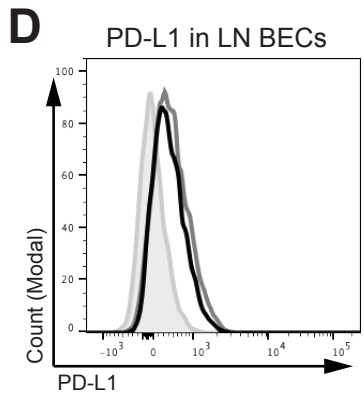

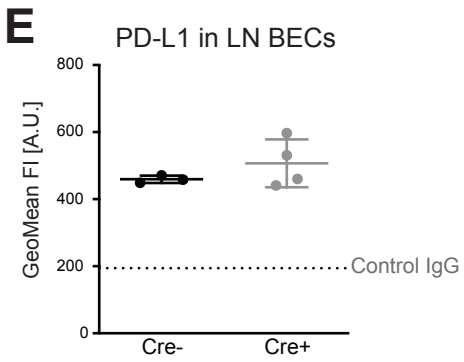

Figure 3

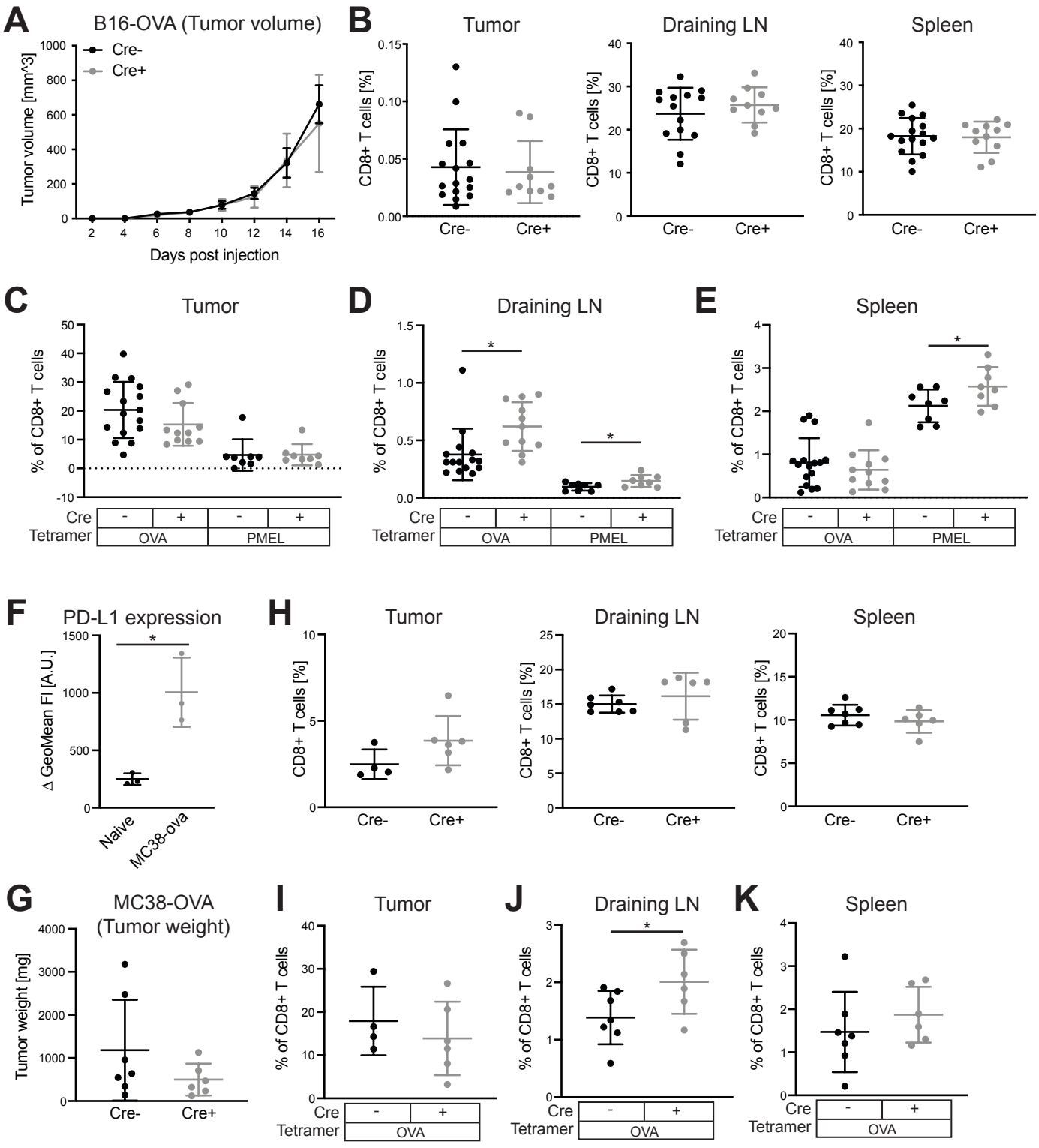

Figure 4

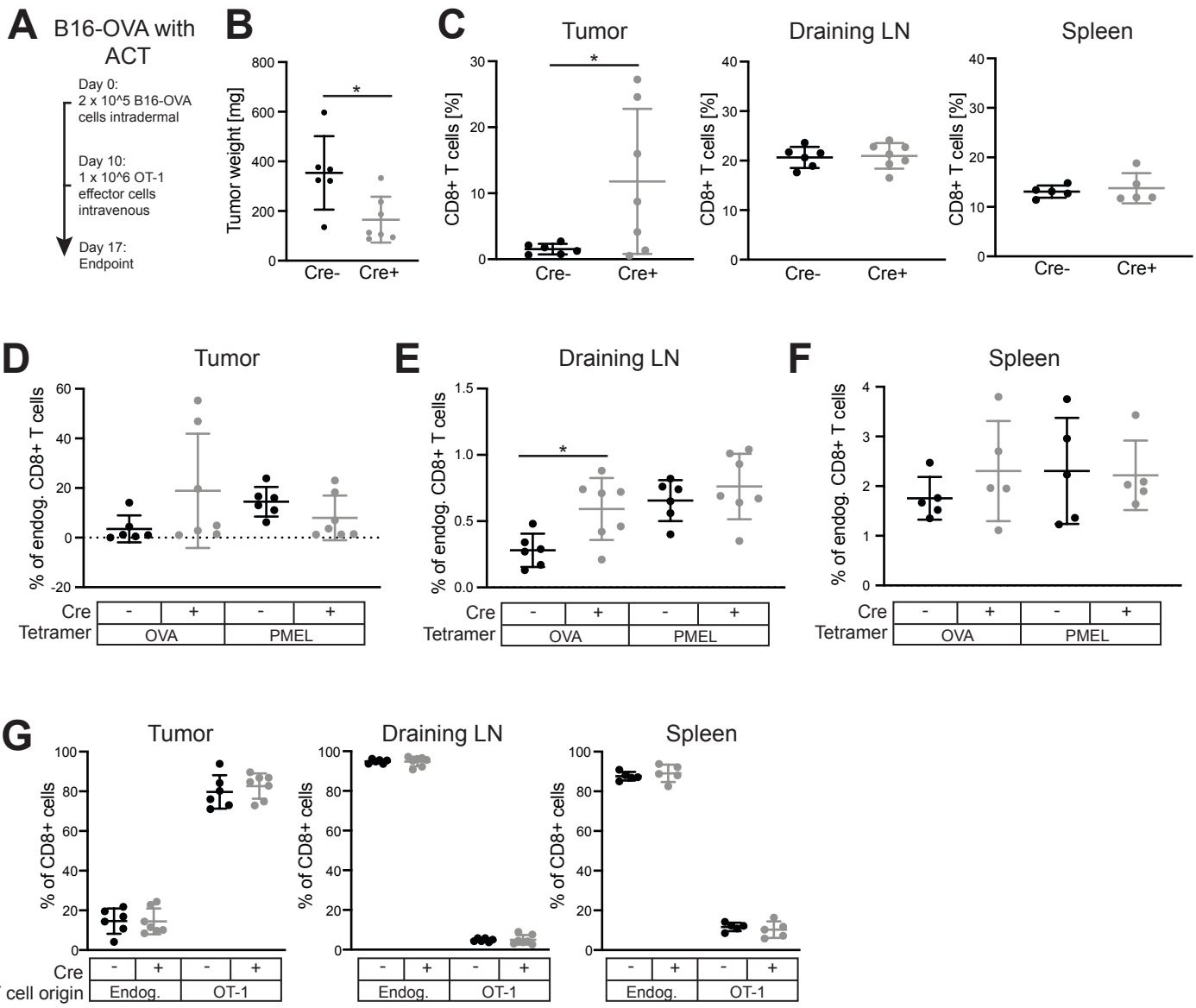

Figure 5